International Journal of Engineering Technology Science and Research
IJETSR
www.ijetsr.com
ISSN 2394 – 3386
Volume 4, Issue 9
September 2017

# Spatial Correlation of a Flare Associated Halo CME on 22 March, 2002 and its Geo-Effectiveness

**Lahkar, M.**
Research Scientist, Centre for Radio Astronomy, Department of Physics
Cotton University, Guwahati, Assam, India
**Saikia, N.**
Associate Professor
Cotton University, Guwahati, Assam, India

**ABSTRACT:**

*The development and radio signature of a flare on 22 March, 2002 has been analyzed using multi wavelength data from ground based as well as space based observations. The successive spatial and temporal evolution of the flare associated CME is found by analyzing NRH radio imaging data and SoHO/LASCO chronographic images. The analysis of the time sequences of the NRH radio images and radio continuum together with Izmiran radio spectrum reveals the existence of distinct phases associated with the evolution of the radio sources, distinct reconnection processes and magnetic restructuring of the corona. An excellent spatial association is found between the position and extension of the magnetic flux loops of the radio source and the CME seen by LASCO. The topology and the evolution of the magnetic flux systems and radio source shows the successive interactions between the different systems of loops. These successive interactions lead to the magnetic reconnection in the small scale and large scale magnetic fields, then to a coronal restructuring. The electrons resulted in these magnetic reconnection leads to the interplanetary radio burst as observed by WIND/WAVES. The analysis of the interplanetary plasma parameters reveals that the CME associated shocks arrives at 1 AU distance after ~60 hours of its initiation and produces moderate Geomagnetic disturbance ~ -100nT.*

***KEYWORDS: Sun, Halo CME, Solar flare, $D_{st}$,***

## INTRODUCTION:

Observations show that solar flare and CME occur often together, and many debates have been arising about their respective relationship. It has not been fully understood about the association between the flares and CME and associated particles. Flares and CMEs are two major manifestations of eruptive energy release with significantly different spatial scales. Usually, flares occur in regions of large scale magnetic fields. Observations provide increasing number of evidences that at least the timing of some CMES are highly associated with flares (Zhang et al. 2001). It is widely believed that the energy released during solar flares is stored in the coronal magnetic fields and flare is caused by the magnetic reconnection. In magnetic plasma with high magnetic Reynolds number anti-parallel magnetic fields are broken and reconnect in an electric current singularity(X-point) that is resolved by magnetic diffusion (Sweet 1958, Parker 1963). In this reconnection process the reconnection inflows and outflows play an important role, carrying the magnetic field lines towards and and away from the X-point. The reconnection model of flare energy release (Priest & Forbes 2000, Kosugi & Somov et, al. 1998) predicts hot reconnection outflow jets surrounded by a system of standing slow-mode shocks in the corona. In the jets surrounded by a system of standing slow-mode shocks called termination shock are expected somewhere between the diffusion region at the top of the post flare loops. Fast mode shocks are usually able to generate energetic electrons and thus possibly also radio emission. Meter-wave radio observations reflect the dynamics of non-thermal energy release (electron acceleration) during solar flares and coronal mass ejections. Several authors have identified (Aurass et al. 2002) radio signatures about 30 minutes after the impulsive phase of a flare as a consequence of fast mode shock.

International Journal of Engineering Technology Science and Research
IJETSR
www.ijetsr.com
ISSN 2394 – 3386
Volume 4, Issue 9
September 2017

However, CMEs are large expulsions of mass and magnetic fields from the sun to the interplanetary medium. It is a large scale or global scale activity. These mass ejection carry a bulk of material of around 1015 gm at a variable speeds ranging from ~100 Km/s to 3000 Km/s (Manoharan et al. 2000). To understand the various manifestation of a CME, it is important to know the spatial and temporal evolution of CMEs and its propagation characteristics in the interplanetary medium. The westward originating CMEs are generally believed to be the primary cause of geomagnetic disturbances which causes the intense Geo-effective solar wind structures. However, not all the earth directed CMEs can produce geomagnetic storms. The evidence has been presented that the properties such as the internal structure of the magnetic field and CME speed determine whether or not a earth directed CME will produce subsequent geomagnetic storms (Burton et al. 1975, Cane et al. 2000).

In this paper, we studied a flare event M1.6 and its associated radio sources and halo CME occurred on 22 March, 2002 on the west limb (S09W90) of the sun during the time period ~10:12–11:52 UT. The flare peaked at 11:14 UT. We analyzed the event using multi wavelength data from various observations e.g. SoHO/EIT 195 Å images, NRH radio imaging data, SoHO/LASCO images and OMNI interplanetary plasma data. The analysis of the event is organized as follows: In section #2 we described the X-ray characteristics of the observed flare using GOES-8 satellite data and MDI magnetogram data for characterizing associated magnetic field structure, different sub-sections in #3 reveals the analysis of Nancay Radio Heliograph imaging data, SoHO/LASCO coronographic images and interplanetary plasma data. In the final section we describe discussion and conclusion of the analysis

## OBSERVATION AND DATA ANALYSIS:

### A. Goes X-ray and MDI images

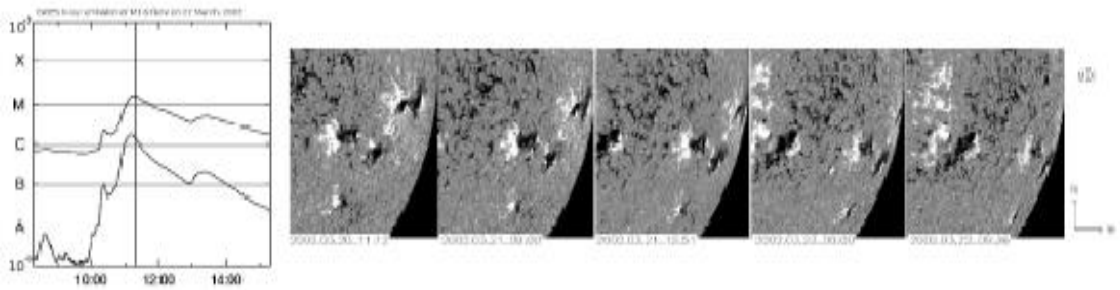


Fig. 1: GOES X-ray flux intensity profile at 1-8°A and 0.5-4°A channels (left) and MDI magneto gram images (right) during the flare on 22 March, 2002

GOES satellite measurements of the soft X-ray shows that the flare on 22nd March, 2002 during 10:12 to 11:52 UT be a typical long duration event lasting about 1 hour 30 minutes and peaked at around 11:14 UT. In figure 1, we have shown the measurements of X-ray emission by GOES-8 satellite in the 1-8 Å and 0.5--4 Å channels. In these intensity profiles clearly show that flare starts rising very fast and within about 30 minutes it reaches its maximum where as post eruptive phase is gradual lasting about 1 hour. These fast and gradual intensity profile shows the involvement of highly sheared large scale magnetic fields as well as small scale magnetic fields reconnection processes. The complexity and strong modification of the destabilized large scale and small scale magnetic field configuration can also be observed in SoHO/EIT images in figure 2.

The active regions (ARs) involved in this event appeared in the east limb with a negative leading polarity on 9 March, 2002 locating at 90. East and 06. South. We studied the AR locations from the date of its appearance at the central meridian on 16 March, 2002. Figure 1(left), shows the MDI magnetogram images which shows that the AR location is very complex and involves a group of sunspots showing strong changes in the flux density as well as its sizes.

International Journal of Engineering Technology Science and Research
IJETSR
www.ijetsr.com
ISSN 2394 – 3386
Volume 4, Issue 9
September 2017

### B. SoHO/EIT IMAGES SHOWING EVOLUTION OF MAGNETIC FLUX

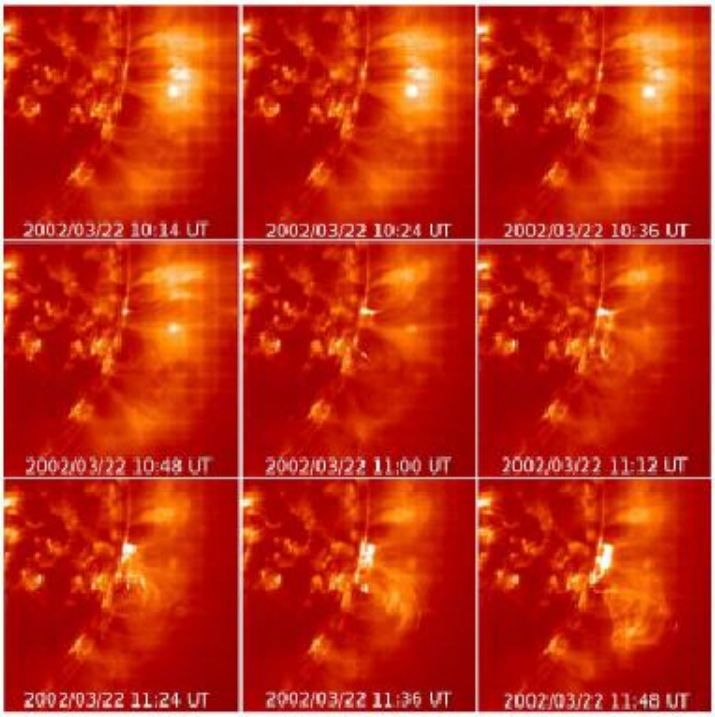


Fig. 2. SoHO/EIT images showing evolution of magnetic flux and location of the radio sources as seen in NRH during the flare

### C. RADIO IMAGING AND RADIO SPECTROGRAPH OBSERVATION

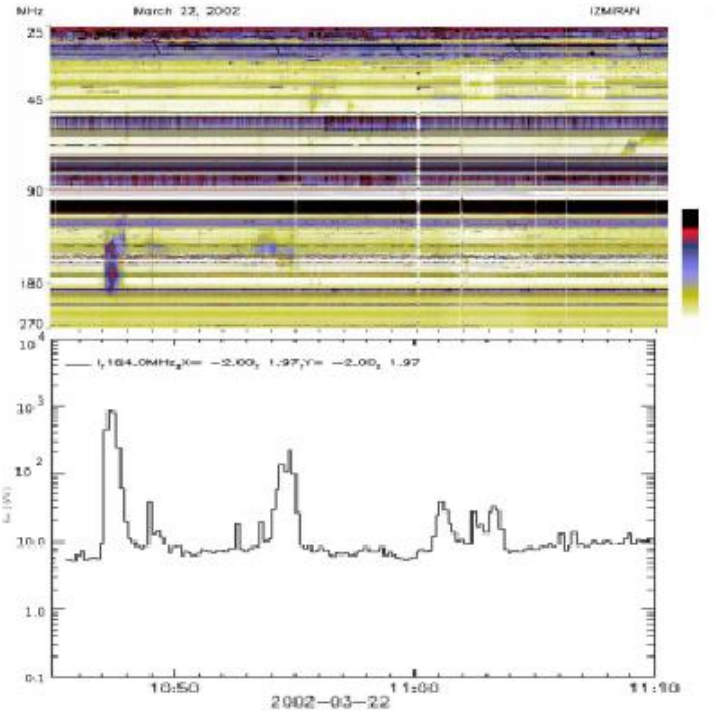


Fig. 3. Izmiran Radio Spectrum (Top) and NRH intensity profile at 164 MHz(Bottom)during 10:45-11:10 UT on 22 March, 2002

International Journal of Engineering Technology Science and Research
IJETSR
www.ijetsr.com
ISSN 2394 – 3386
Volume 4, Issue 9
September 2017

The various stages of this eruptive event are studied by using two dimensional radio imaging data from Nancay Radioheliograph (Kerdraon & Delouis 1997) and Radio spectrograph( Gorgutsa et al. 2001) data from Izmiran Solar Radio Laboratory. The high time resolution images are routinely made at the Nancay Radioheliograph (NRH), which operates in the frequency range of 150–435 MHz and probes the sun's coronal plasma at a height of ~< 1.5 $R_o$. Izmiran radio spectrograph observes the radio spectra of the coronal transient events in a frequency range of 270–25 MHz, which corresponds to the radio emission from the lower corona to the interplanetary medium. In figure 3, we have shown NRH 164 MHz flux profile and Izmiran radio spectra during the eruptive event.

The radio emission following the sudden flux enhancements during the event and is composed of a series of type III and intense type II radio bursts followed by type I continuum. The radio spectra as observed by Izmiran reveals the coronal plasma conditions and the NRH radio images show the expansion and evolution of radio source during the time of enhanced radio flux emission. The observations in the NRH radio imaging and the radio spectrum reveal that a fast drifting type II burst observed ~10:47 UT in the frequency range of 220-130 MHz. The intensity of the burst as measured by NRH is ~1000 SFU (1SFU = $10^4$ J ). There is a group of type III bursts observed by the spectrograph, which also starts around 220 MHz, continuing up to ~110 MHz during 10:47 UT. The type I continuum revealed by the Izmiran spectrograph observed during the time interval of 10:48:03–10:49:09 UT in the frequency range of 150-110 MHz.

The source location of type II metric radio bursts are derived from the NRH radio images. Both fast drifting type III and type II radio burst seen in the dynamic spectra of Izmiran have revealed from the appearance of the radio sources in the NRH images. The spatial evolution of the NRH radio source can also be seen from the EIT 195 Å images as shown in figure 2.

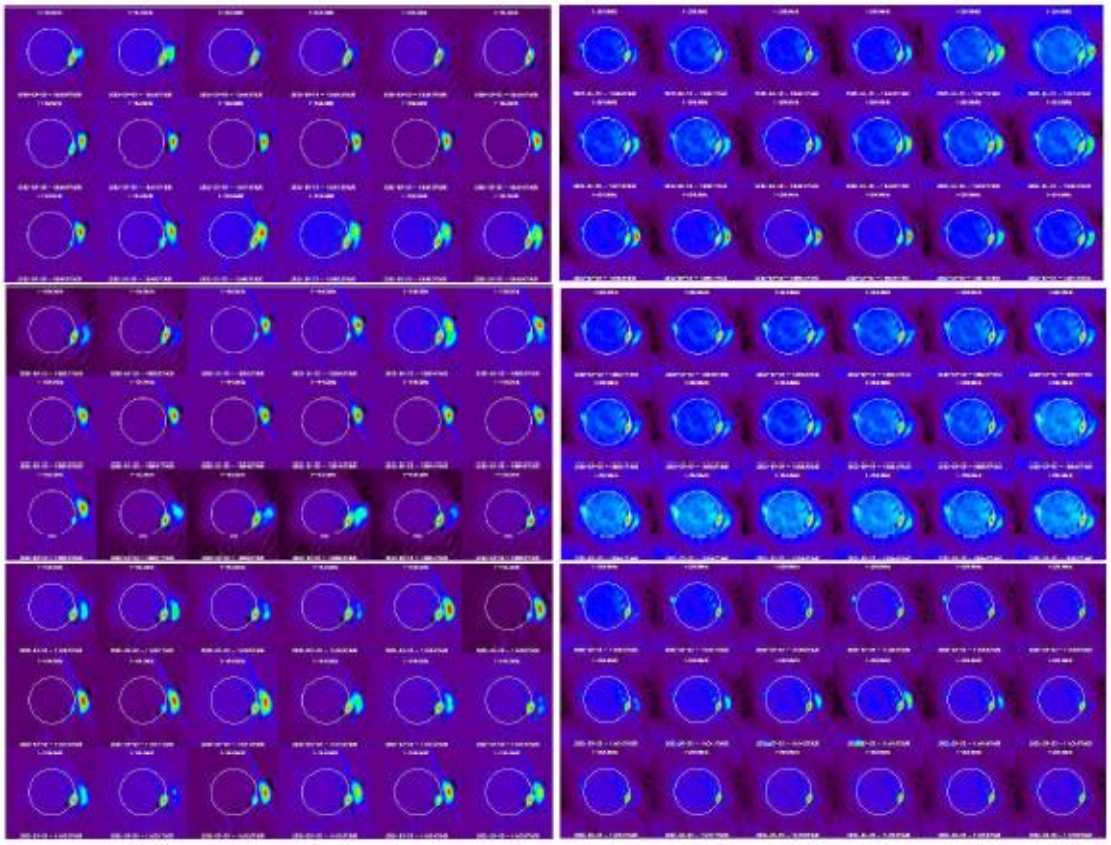

Fig. 4. NRH images showing the spatio-temporal evolution of the radio sources during the out bursts at ~10:45-11:04 UT

International Journal of Engineering Technology Science and Research
IJETSR
www.ijetsr.com
ISSN 2394 – 3386
Volume 4, Issue 9
September 2017

Figure 4, shows the spatio-temporal evolution of the radio images of NRH at 164 and 236 MHz during the successive radio bursts. One can distinguish the following district phases of the radio burst observed in the flux profile of the NRH at 164 MHz : the first one which starts at around 10:46:47 UT and ends at 10:50:00 UT corresponds to an out bursts last for about 100s. Before the end of this out burst there is an intense type III radio burst which followed by a short duration type I continuum(as shown in fig 3). The second phase of the radio bursts starts at ~10:52 UT with a very short duration radio spikes and end at ~10:55 UT. After the second phase there is a short sporadic radio burst observed which corresponds to another type I radio continuum. At ~11:00 UT the third phase of radio bursts is observed with three distinct peaks and this phase last up to 11:04 UT which corresponds to the initiation of the coronal mass ejection (CME) as seen later in SoHO/LASCO coronographic images. The details of the out bursts observed in NRH imaging observations are discussed below.

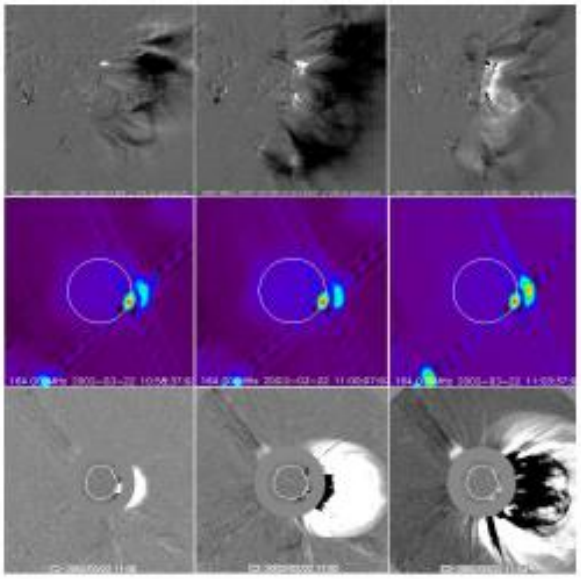

Fig. 5. EIT running subtracted (top), NRH(middle) and LASCO(bottom) images showing the successive spatial evolution of the CME

In figure 4, shows the spatio-temporal development of the successive radio sources. In the early development of the first phase of radio out bursts a series of short bursts are observed in the NRH flux measurements. After about 10:46:47 UT the out burst starts as seen in fig 3. This out burst which is also observed with the Izmiran radio spectrograph corresponds to the radio burst of type III overlapped on a fast drifting type II radio burst. The spectrograph reveals a complex radio emission of fast drifting fundamental and second harmonic emission. The emitting region is composed at two frequencies 164 MHz and 236 MHz. It shows one main source at south-west quadrant and additional extended source towards north-west over the main source and appears up to 10:48:57 UT from 10:46:47 UT. Few seconds after the appearance of the additional extended source the main source disappeared at 164 MHz frequency, but still visible at 236 MHz. The additional source shows its expansion during type II development towards north-south direction. The main source which was disappeared at 164 MHz for a few seconds reappeared again at ~10:47:57 UT and its starts expand towards additional north-south source and merged with it showing structure like number 8. The merged sources are again separated at 10:48:27 UT and the main source shifted slightly above its original position.

The additional source reappears in its previous position with greater extension than the previous size. The intensity of this additional source lasts for a few seconds and again disappears at around 10:50:17 UT. Since the active region location is almost behind the limb, the NRH high frequency observations corresponding to the plasma emission ~<= 1 $R_0$ are blocked by the limb in the line of sight and hence the side lobes are more prominent than the main radiation pattern in these frequencies, hence they look interfered.

International Journal of Engineering Technology Science and Research
IJETSR
www.ijetsr.com
ISSN 2394 – 3386
Volume 4, Issue 9
September 2017

The development of the second phase of the radio burst starts at 10:52:17 UT and last up to 10:54:30 UT in both the frequencies. In figure 4, NRH images show that just before few seconds of the development of this burst there is a faded source above the main source as mentioned earlier, which corresponds to the short duration type III like spikes and this source is visible till the last of the burst at 236 MHz. The development and extension of this burst source can be seen distinctly at 164 MHz images, which shows reappearance of the additional source as mentioned in the first phase of radio bursts. The expansion of this source starts at 10:52 UT in the north-south direction and evolves as a large expanded source at 10:53:47 UT and then compact to its original size within a few seconds. The main component of the extended source remains detectable until the end of this burst phase then after it disappeared. The shape and position of the additional source remain constant for a long interval of time of this burst. We are observing the complexity and strong modifications of the emitting source in the EIT movie during this time interval. After this out burst EIT 195 Å images show the coronal restructuring of the magnetic loops and evolution of a new flux rope like structure during 11:00 to 11:06 UT as shown in fig 2. High temporal evolution of the magnetic flux systems associated with the radio sources are not possible with EIT since observation cadence is very low, but we are very fortunate that the image frames observed in EIT is well corresponds to the NRH bursts related radio source images.

The third phase of the radio burst starts at 11:00 UT in the NRH flux profile which shows the progression of the CME associated flux rope as observed later in SoHO/LASCO images. There is an excellent agreement of the spatio-temporal evolution of the CME between NRH images and LASCO coronographic images. In the LASCO C2 field of view, CME is first appeared at 11:06 UT. In figure 4, the NRH images during 11:00:47 UT shows the evolution of the extended radio source above the active region and later on radio source shows its greater separation from the main source and then expand, which corresponds to the propagation and expansion of the CME into the interplanetary medium. Fig 5, displays the composite images, showing the spatial correspondence of the CME evolution in EIT, NRH and LASCO observations. There is no distinct radio signature in the Izmiran spectrograph during the evolution of CME. In the NRH flux profile during 11:00 to 11:04 UT we observe single peak short duration outburst and a double peak long duration out burst which are likely to be corresponds to the interplanetary type III and type II radio burst as observed by WAVES/Wind. In the NRH images during 11:00:47 to 11:01:27 UT the radio source expands and slightly shifted to high altitude and then faded in its intensity during 11:01:47 to 11:02:17 UT which corresponds to coronal restructuring and initiation of the CME. Again the source intensity increases and shows the oscillation in its extent and intensity. After about 11:03:47 UT the extended source disappeared.

### D. INTERPLANETARY RADIO SIGNATURES OF THE CME

The WAVES/Wind experiment (Bougeret et al. 1995) observed the CME features at the whole frequency range as a type II narrow band radio burst recorded in the dynamic spectrum of the high frequency radio receiver RAD2. The operation frequency of RAD2 is in the range of 1.075 to 13.825 MHz. The corresponding wavelength range is referred to as DH regime(Raymond et al. 2000, Kundu & Gopalswamy 1992). Figure 7, dynamic spectrum of the

Fig. 6. LASCO images showing the evolution of CME in C2 and C3 field of view and speed-height plot

International Journal of Engineering Technology Science and Research
IJETSR
www.ijetsr.com
ISSN 2394 – 3386
Volume 4, Issue 9
September 2017

event from 11:04 to 12:05 UT on 22nd March, 2002. The event was marked by WAVES/Wind observation as intense type III -like burst (the intense vertical feature) during 11:12 to 11:25 UT, followed by intense narrow band type II burst (the slanted feature) with obvious fundamental and harmonic structure. The type II burst shifted in frequency and shows the much intense fundamental than the harmonic. We examine the association of DH type II radio bursts with white light images of the corona from LASCO observation (Brueckner et al. 1995). The figure 8, shows the evolution of the CME in LASCO C2 and C3 field of view and corresponding CME speed-height plot into c2 and C3 field of view. The observed CME speed in the LASCO C2 field of view is 1750 Km s-1 and 1685 Km s-1 from the second order fit in the LASCO CME catalog. The CME with such a high speed indeed associated with DH type II burst. At decimetric-metric wavelengths no clear type II emission is found as seen in Izmiran dynamic spectrum. At DH wavelengths observed by WAVES/Wind type II burst drift with a rate of 1.5 MHz $s^{-1}$ and shows the lane of fundamental frequency at 4 MHz see in fig 7, which lane of fundamental frequency at 4 MHz see in fig 7, which corresponds to the plasma density of 2 x $10^5$ particles $cm^{-3}$ according to the Saito density model, it corresponds to the atmospheric height of ~7.09 $R_o$ which agree with the LASCO CME height ~7 $R_o$ at 11:30 UT. Using these model parameters for type II during 11:30 to 12:30 UT we found the speed of the type II driver shock is ~2500 Km $s^{-1}$ at a height of ~7 $R_o$. It shows that the calculated shock speed corresponds to the observed CME speed.

### E. GEO-MAGNETIC STORMS OF THE ASSOCIATED HALO CME

The association of the geomagnetic storms caused by the observed limb halo CME (S09W90) is examined using 1AU interplanetary plasma data. Figure 8, shows the ecliptic north-south component (Bz) of the IP magnetic field (IMF), solar wind plasma temperature (T), and the plasma pressure (P) for determining the sheath and ejecta portion of the CME and the corresponding storm index (Dst). We have investigated all other CME during the time window of the limb halo CME, which may also cause of geomagnetic storms during that time range. We found two probable CMEs occurring at the same active region location one of which is disk halo during 17:54 UT and other one during 23:54 UT on 20th March, 2002 with an angular width of ~>160 at position angle 243.. The corresponding speed of the CMEs are 603 km/s (declaration ~-15.8 Km/s) and 1075 km/s (deceleration ~ -0.2 Km/s) respectively and propagating towards southward direction. All these CMEs are associated with

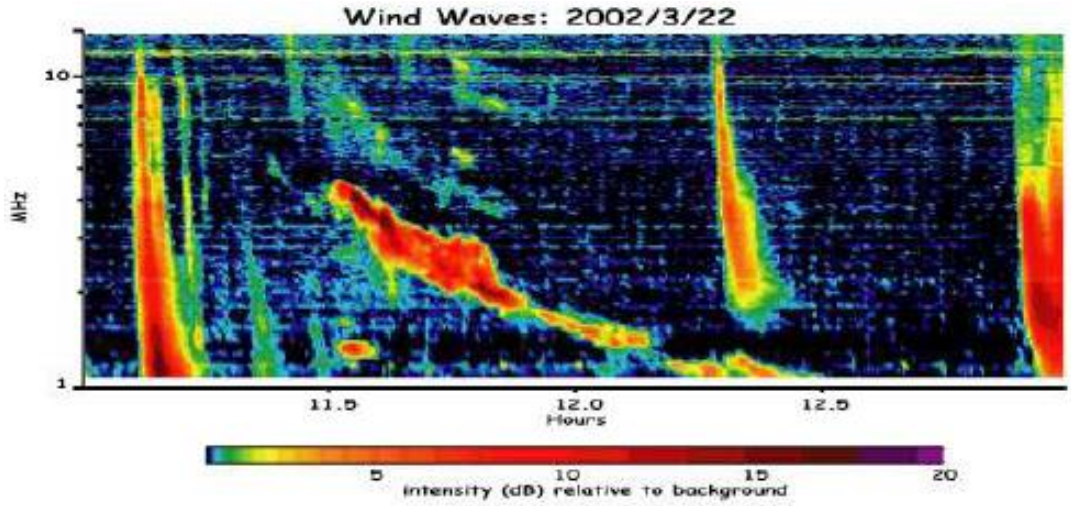


Fig. 7. WAVES/Wind dynamic radio spectrum during 11:00-12:30 UT

interplanetary type II bursts which indeed associated with shock ahead of the ejecta. It is widely accepted that the arrival time of the shock and ejecta is in the time range of 1 to 4 days, and 1AU arrival time delay between the shock and CME associated with each individual CME is ~10 hours (±2 hours). In fig 9, we are showing the extrapolated height-time plot of these three CMEs from near sun to 1 AU distance using SoHO/LASCO

International Journal of Engineering Technology Science and Research
IJETSR
www.ijetsr.com
ISSN 2394 – 3386
Volume 4, Issue 9
September 2017

and interplanetary scintillation observation, which reveals that possibly two halo CMEs (disc and limb halo CME) interact each other near 1AU distance. During this interaction the IP shock associated with the limb halo CME seems to pass through the ejecta of the disc halo CME, but the IP shock associated with the CME at 23:54 UT is moving ~12 hours ahead of its ejecta, therefore it doesn't have any impact with the preceding CME at 11:06 UT on 22 March, 2002. The ecliptic southward component ($B_Z$) of the magnetic field associated with the sheath region of 23:54 UT CME on 20 March, 2002 and the ejecta region of the CME at 11:06 UT on 22 March, 2002 can easily be identify from figure 8 and its corresponding Dst value. It clearly shows that the Dst due to the sheath region is more stronger than the ejecta of the CME at 11:06 UT, which determines by the southward component ($B_Z$ <0 or = 0) of the IMF associated with Sheath or ejecta.

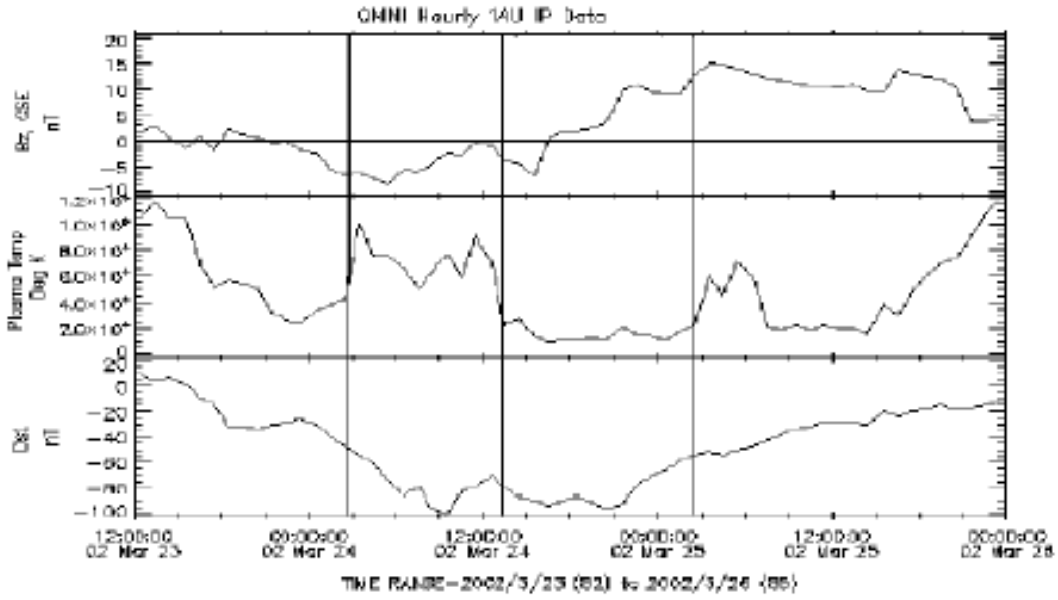


Fig. 8. 1 AU interplanetary parameter for determining Geo-effectiveness of the associated CME shock and ejecta

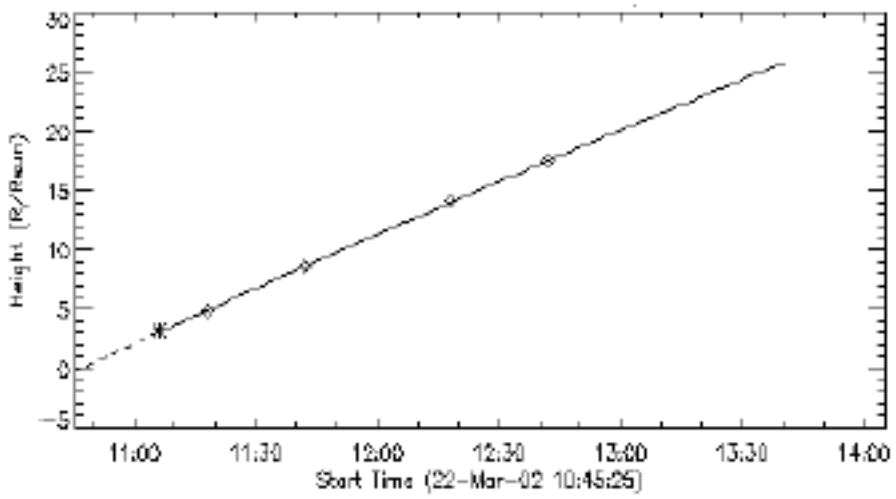


Fig. 9. CME height-time plot extrapolated backward

International Journal of Engineering Technology Science and Research
IJETSR
www.ijetsr.com
ISSN 2394 – 3386
Volume 4, Issue 9
September 2017

## DISCUSSION:

The observations and analysis of the time sequences from the various observational data reveals that the initial instability of the magnetic field starts at ~09:36 UT, when the first type III and sporadic radio burst of type I are observed. The evolution of the type II burst starts in the same region with two distinct component of the source, i.e. main and additional source as referred earlier, at the same time when type III bursts are observed. The present study reveals the association between the type II exciter and the fast mode shock ahead of the coronal jet. The formation of the streamer is observed at the same altitude after the jet in the EIT images, which reveals the restructuring of the coronal magnetic field as due to the passage of the shock. The signature of the type III burst is also an evidence of the magnetic field reconnection and restructuring the coronal magnetic field. A clear and excellent association is found between the NRH flux enhancements and the modifications of the source structure.

The topology and expansion of the emitting source, which are observed during the flux enhancement, suggest the evolution of a new rising magnetic flux and its interactions with other magnetic loops. EIT observations clearly show these rising arches and the interactions with other small scale and large scale magnetic loops. The high frequency radio observations can only show the interactions which starts at low altitudes, but unfortunately we do not have high frequency observation due to interference in NRH high frequency data. The magnetic field becomes progressively open, and the interaction can occur at high altitudes, becomes detectable at lower frequency as already suggested(Manoharan et al. 1996, Buttingho_er et al., 1996). Therefore, the enhancement we observe at 164 MHz corresponds to high altitude. The radio enhancement observed at 164 MHz is due to the accelerated electrons resulted from the interactions; therefore this study reveals that the accelerated electrons can have the source at higher altitudes due to the large scale magnetic field interactions. This study supports the explanation of Robinson (1986) who suggested that this type of radiating particles is accelerated by the shock formed at the leading edge of the transient.

The indications of expansion seen in radio observations suggest that the CME has already reached velocities of a few Km/s in the low corona. In figure 10, we have shown the extrapolated plot of the CME height-time plot in C2 and C3 field of view. The back extrapolation of this height-time plot intersects the CME height and time ~7 Ro at 10:54 UT, which reveals the time of radio burst as observed by NRH and its corresponding height ~7 Ro. Therefore, we confirm that the radio signature at 10:54 UT observed by NRH is the first radio signature of CME initiation.

In our present study we found that the multiple Geo-effective CME were occurred from the same active region location during the time window of the limb halo CME (S09W90). The Geo-magnetic storm is associated with the ejecta portion of the ICME on 22$^{nd}$ March, 2002 and corresponding delay time is ~60 hours from the CME initiation to the observed Dst index. The study reveals that the CME is not directed along the shortest sun-earth line and only a partial part of the CME hits the earth's magnetosphere. The observed $B_z$ value is also the evidence of small width ejecta. We also infer that proceeding slow CME can decrease the strength of the Geo-effectiveness when it pass though the ejecta of the slow CME. The more effective Dst can produce by the sheath of the ICME then the high speed ejecta as observed in the present study, probably due to the associated southward component of the IMF.

## CONCLUSION:

***ACKNOWLEDGEMENT:*** Authors are grateful to Assam Science Technology & Environment Council, Govt. of Assam and Eastern Centre for Research in Astronomy (ECRA), Kolkata sponsored by the UGC, Govt. of India for the fund provided time to time to the Centre for Radio Astronomy, Department of Physics, Cotton College, Guwahati, Assam, India. Authors also thank to the all the Researchers at the Radio Astronomy Centre, Ooty, NCRA-TIFR, for their valuable help in documentation of this article.

**REFERENCES:**

[1] Aurass, H., Hofmann, A.Vrsanak, B 2002 in Solar Variability. From Core to Outer frontiers, ed. J. Kuijpers, ESA Special Publication, 506, 423
[2] Bougeret, J.-L., Kaiser, M.L, Kellogg, P.J., et al. 1995, Space Science Revews, 71, 231
[3] Brueckner, G.E., Howard, R.A., Koomen, M.J., et al. 1995, Solar Physics, 162, 357
[4] Burton, R.K., McPherron, R.L., Russel, C.T., 1975, JGR, 80, 4204
[5] Cane, H.V., Richardson, I.G., Cyr, O.C.S. 2000 GRL, 27, 3591
[6] Kerdraon, A., Delouis, J.,-M., 1997 in Coronal Physics from Radio and Space Observations, ed. G. Trottet, Lecture Notes in Physics, Berline Springer Verlag, 483, 192
[7] Kosugi, T., Somov, B. 1998, in Observational Plasma Astrophysics: Five Years of YOHKOH and Beyond, eds. T. Watanabe & T. Kosugi, Astrophysics and Space Science Library, 229, 297
[8] Kundu, M.R., Gopalswami, N. 1992, in IAU Colloq 133. Eruptive Solar Flares, eds. Z. Svestka, B.V. Jackson, & M.E. Machado, Lecture Notes in Physics, Berline Springer Verlag, 399, 268
[9] Manoharan, P.K., Kojima, M. Gopalswami, N., Kondo, T., Smith, Z., 2000, ApJ, 530, 1061
[10] Manoharan, P.K., Van Driel-Gesztelyi, L., Pick, M., Demolin, P., 1996, ApJ, 468, L73+
[11] Parker, E.N. 1963, ApJS, 8, 177
[12] Zhang, J., Dere, K.P., Howard, R.A., Kondo, M.R., White, S.M. 2001, ApJ, 559, 452
[13] Preist, E., Forbes, T. 2000 Magnetic Reconnection, ed. E. Priest& T. Forbes